International Journal of Research Publication and Reviews

Journal homepage: www.ijrpr.com ISSN 2582-7421

In-Vitro Studies on Velocity Profile, Flow Rate and Flow Type in the Common Carotid Artery Using B-Mode Doppler Ultrasound

Pam S.D [1]*(PhD), Dakok K.K[2] (PhD) Sirisena A U.I[1](PhD), Nabasu S.E [2] (MSc)

[1]Jos University Teaching Hospital Jos, Plateau State, Nigeria, [2]Department of Physics, Plateau State University Bokkos, P.O Box 2012, Plateau Sate, Nigeria

Corresponding Author: dakokkyense@gmail.com

Abstract

Objective: Blood flow in elastic tubes and vessels is a complex pulsatile flow of non-homogeneous fluid, hence understanding its physical properties is very important when studying images from colour flow Doppler spectra. This study is aimed at studying velocity profile and flow pattern in the common carotid artery by the use of a wall-less phantom. **Method:** The phantom was constructed with common carotid artery (CCA) lumen diameters of 4.5-8.0 mm within normal human carotid geometry. The tissue mimicking material (TMM) consists of konjac, carrageenan and gelatine as basic components mixed with other suitable components. The blood-mimicking fluids (BMF) were prepared by mixing propylene glycol and Glucose, while poly 4-methystyrene and cholesterol serve as scattering particles. The constructed phantom was scanned using ultrasound machine to measure the mean flow velocities through the lumen. **Results:** Mean velocity values were detected and recorded for flow rates from 500 ml/min up to a maximum of 1500 ml/min, above this maximum flow rate; velocity measurements were not possible. For each flow rate, velocity values increased from 8.0 mm diameter to 4.5 mm diameter phantoms, while for each diameter phantom, the velocity values increased with increase in the flow rates. Good velocity profiles were obtained with flow assessed to be laminar. **Conclusion:**Since laminar flows and good velocity profiles were established across all lumens in the phantom in this research, we can conclude that studies on V_m, velocity patterns and flow types in the CCA can be studied using wall-less phantoms by Doppler ultrasound method

Keywords: Tissue Mimicking Material; Blood Mimicking Fluid; Common Carotid artery; Mean Flow Velocity; Flow Rate; Velocity Profile.

INTRODUCTION

Velocity measurements and changes in Doppler spectrum help in identifying and assessing disease severity. Basically, there are two types of fluid flow known as laminar or streamlines flow and turbulent flow. For a laminar flow (flow in normal arteries at rest), the layers move in a parallel direction without disruption, but at high velocities caused by stenosis or stiffness of the vessel, the flow becomes turbulent (Batten & Nerem, 1982; Peter *et al.*, 2019). In turbulent flow, particles follow irregular and erratic paths, with their velocity vector varying continually both in magnitude and direction.To differentiate between laminar and turbulent flows in blood vessels, a dimensionless quantity known as Reynold's number represented by Re is very important. This quantity relates four basic quantities such as the velocity, viscosity of the liquid (blood), density and the diameter of the vessels written mathematically in equation 1(Batten & Nerem, 1982; Peter *et al.*, 2019)as:

$$\mathrm{Re} = \frac{\rho v d}{\mu} \quad \ldots\ldots\ldots\ldots\ldots\ldots\ldots\ldots\ldots\ldots\ldots\ldots\ldots\ldots\ldots\ldots\ldots\ldots\ldots\ldots \; 1$$

Where ρ is the density of blood, v is the mean velocity of blood, μ is the viscosity of blood and d is the diameter of the blood vessel. A Reynold's number of less than 2300 defines laminar flow, while a number higher than 4000 is characterized by a turbulent flow (Philip *et al.,* 2016). Reynold's number of smaller vessels such as the capillaries is very low resulting to laminar flow instead of turbulent flow; this is because of the smaller values of their diameters and velocities compared to other vessels.

Steady and unsteady flows originate from laminar and turbulent flows. A steady flow is one in which all conditions (such as velocity and pressure) at any point in a stream remains constant with respect to time, while turbulent flow may never be described as steady as there are variations in both velocity and pressure at every point. However, the definition is usually expanded to include flow in which the conditions fluctuate equally on both sides of a constant average value (Caro *et al.,* 2012). A steady flow in rigid tubes is well understood as a convenient discussion of blood flow in arteries. It is also relevant because pulsatile flow can be considered to be the sum of a steady component and a number of oscillatory components which interact neither with each other nor with the steady component.

Disturbed flow on the other hand refers to regions of circulating flow and reversal in flow commonly attributed to the distal part of an atherosclerotic plaque (Peter *et al.,* 2019). However, the presence of disturbed flow does not by itself signify the presence of disease and may be seen in a normal bifurcation. For instance, flow reversal in the carotid bifurcation is known to be a normal result.Blood flow within a vessel does not have the same velocity at any given time. It is faster at the centre of the vessel and slow near the vessel wall due to viscous drag exerted by the walls causing the fluid at wall to become stationary. This difference in the flow velocity across the vessel is referred to as velocity profile. As a homogeneous fluid enters a

long tube with a steady flow, it moves from a blunt flow profile with all the fluid moving with the same velocity to a parabolic flow(Caro *et al.,* 2012). As a fluid flows through a tube, it moves for a given entrance length before it arrives at its steady-state velocity profile. The viscous drag upon the walls of the tube (vessel) is transmitted to the central part of the tube by a progressive growth of regions of shear stress or boundary layers. Initially, only the fluid directly in contact with the wall is stationary, and a large velocity gradient is present at this point.

The distance over which the velocity profile transits from blunt to parabolic flow is dependent on the diameter of the vessel and velocity of the fluid, but the velocity is usually several times the tube diameter. The same difference in velocity profile is observed in several vessels in the human body, for instance, flow profile up the aorta is blunt while it is parabolic in the normal mid superficial femoral artery even though the shape of the velocity profile can be complicated by the pulsatile nature of blood flow (Peter *et al.,* 2019).In arteries, blood flow is pulsatile and the velocity profile varies over time, therefore, for normal common femoral arteries and common carotid arteries, there is no reverse flow except during diastole where reverse flow is observed in the common femoral artery. The velocity profile is also affected at branches and curves. It is asymmetric at the proximal internal carotid artery (ICA) with a high velocity flow occurring towards the flow branch and a reverse flow happening near the wall away from the origin of the external carotid artery (ECA) depending on the geometry of the bifurcation area.

The Velocity profile in a vessel can be affected if the artery is having a disease. The velocity of blood flowing through a stenosed portion of an artery will be increased because the lumen has been narrowed by the presence of the disease. As the blood passed beyond the stenosed area, the lumen becomes expanded which may cause a reversal in the flow (Caro *et al.,* 2012). These high velocity flow profile around the narrowed area and the reversal encountered beyond the stenosed area are usually observed with the aid of a colour flow ultrasound at the site of the main stenosis. Information on velocity changes in blood flow across the narrowing of arteries is used to dictate the presence of stenosis and the degree to which it has affected the artery usually under a spectral Doppler investigation. The use of velocity changes as criteria to dictate any reduction in the lumen of a vessel is a more sensitive method compared to blood flow measurements. This is because flow reduction is only noticed when there is a significant reduction in the lumen despite the velocity increase at any level of lumen narrowing(Merrilee & Judith, 2020; Sandra, 2018). A point will reach during the narrowing of the lumen such that the blood flow will drop to an extend that the velocity begins to decrease and a stream-line (trickle) flow is noticed within the vessel

The literatures described above were done by in-vivo means, it is expedient to study same by in-vitro method to be used in clinical setting especially for quality testing purposes and for training of operators in the field of ultrasound. This research aims at comparing results obtained by in-vitro method with those gotten by in-vivo means on the nature of velocity flow profile, flow rate and flow types in the Common Carotid Artery (CCA). An acceptable comparison can reduce the dependence on using humans for researches on blood flow in the carotid artery.

MATERIALS AND METHODS

2.1 Materials: The material required for this research are made up of chemical items and apparatus needed to prepare blood mimicking fluids and CCA wall-less phantom. Chemicals used for preparing BMF include propylene glycol (PG), polyethylene glycol (PEG Mw 200), D(+)-Glucose (DG),total cholesterol, Poly (4-methylstyrene)and Benzalkonium Chloride (BKC)all purchased from Sigma Aldrich company. Items needed to prepare a tissue mimicking material (TMM) for the CCA wall-less phantom fabrication include; Silicon Carbide Powder, Aluminum Oxide, gelatin,conjac root glucomannan powder,carrageenan powder, Potassium Chloride and glycerol also gotten from Sigma Aldrich.

2.2 Methods

The first Stage involved in this section was the preparation of a blood mimicking fluid (BMF) whichwas produced by mixing 0.8% w/w of poly 4-methylstyrene with the mixture fluid (5% w/w of PG, 11% w/w of DG and 84% w/w of water). Another BMF was prepared by mixing 0.70 % of cholesterol scatters with, 17.37% w/w of DG by weight, 5% w/w of PG, and 77.63% w/w of distilled water (Dakok*et al.,* 2021). A CCA wall-less phantom with 8 different sizes of lumen diameters was fabricated by constructing a phantom box followed by preparing the tissue mimicking material (TMM) and finally, casting the TMM inside the phantom box. The TMM adopted for the wall-less phantom in this research is the Konjac-Carrageenan (KC) and gelatin based mimicking material (Ammar *et al.,* 2018) with its constituents shown in table 1.

Table 1: Constituents of Konjac-Carrageenan (KC) and gelatin (from bovine skin) tissue mimicking material (TMM) for wall-les phantom

Name of substance	Percentage Composition (%)	Function
Distilled water	84.0	Serves as water component of the tissue
Silicon Carbide	0.53	Serves as scatters
Al_2O_3 powder (3 μm)	0.96	Serves as scatters
Al_2O_3 powder (0.3 μm)	0.89	Serves as Scatters
Konjac powder	1.5	For gel formation
Carrageenan powder	1.5	For gel formation
Potassium Chloride	0.7	To fertilize the TMM
Glycerol	9.0	To mimic the acoustic properties of the tissue
Gelatin	0.92	To make the TMM strong
50% Benzalkonium Chloride		Preservative

The densities of the BMF fluids samples were measured using a portable Density Meter (DMA 35), while their viscosities were measured using an electronic rotational viscometer (ERV). The speed of sound, attenuation and back scatter power of the BMF and TMM were measured by pulse echo (PE) method using the A-scan Gampt machine.

A digital clinical Hitachi ultrasound scanning machine connected with a linear array transducer (EUP-L74M) with frequencies ranging from 5 to 13 MHz (figure 1) was used to get image information from vascular wall-less flow phantom(Colquhoun *et al.,* 2005; Kenwright *et al.,* 2015; Zhou *et al.,* 2017; Hwang, 2017). Measurements of the mean flow velocities (V_m) for both BMF samples were carried out by colour Doppler and Pulse- wave (PW) Doppler systems and results were recorded.

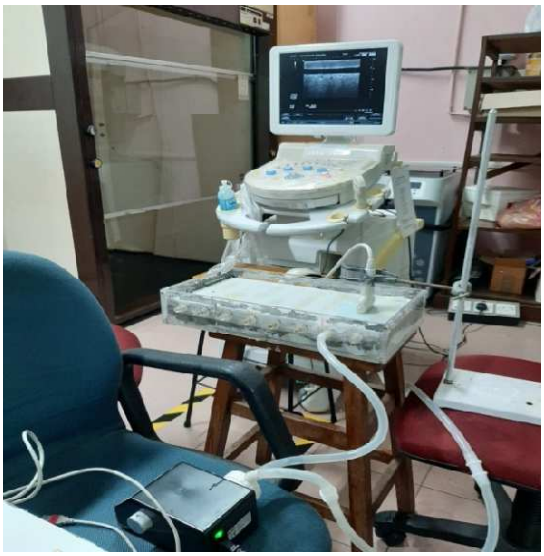

Figure 1: Ultrasound measurements of hemodynamic parameters using the Hitachi ultrasound machine

Results and Discussion

3.1 Variation between BMF Mean Velocity with Flow Rate

Flow velocities of BMF samples could not be detected by the ultrasound machine for flow rates from 100 ml/min to 400 ml/min through the entire 8 wall-less phantoms. This may be due to small volume of flow per minute making it not possible to detect such slow velocities. Velocity values were detected and recorded for flow rates from 500 ml/min up to a maximum of 1500 ml/min, above this maximum flow rate; velocity measurements were not possible as well. Tables 2 and 3 show the results of mean velocities for the flow rates from 500 – 1500 ml/min for BMF with glucose and with cholesterol respectively. For each flow rate, velocity values increased across 8.0 mm diameter to 4.5 mm diameter phantoms, while for each diameter phantom, the velocity values increased with increase in the flow rates (Correia *et al.,* 2016). Therefore, for other hemodynamic measurements, flow rate was maintained at 1500 ml/min being the maximum flow rate for the phantoms.

Table 2: Mean velocity measurements of BMF with glucose for flow rates from 500 – 1500 ml/min across the 8 wall-less phantoms.

$V_m(\pm 0.10$cm/s)/ Flow Rate	500 ml/min	700 ml/min	900 ml/min	1100 ml/min	1300 ml/min	1500 ml/min
8.0 mm Diameter	12.2	19.8	26.0	31.3	38.9	48.2
7.5 mm Diameter	15.5	23.7	30.0	37.3	44.8	49.3
7.0 mm Diameter	17.3	26.4	35.1	42.9	46.8	49.3
6.5 mm Diameter	21.0	31.4	39.8	48.5	50.2	54.4
6.0 mm Diameter	24.8	35.4	46.5	55.7	62.3	69.9
5.5 mm Diameter	29.8	40.3	52.4	60.9	65.7	73.5
5.0 mm Diameter	35.6	46.2	64.7	72.8	77.9	82.2
4.5 mm Diameter	44.3	55.6	68.5	75.9	80.0	83.5

Table 3: Mean velocity measurements of BMF with cholesterol for flow rates from 500 – 1500 ml/min across the 8 wall-less phantoms.

Vm((±0.10cm cm/s)/ Flow Rate	500 ml/min	700 ml/min	900 ml/min	1100 ml/min	1300 ml/min	1500 ml/min
8.0 mm Diameter	8.6	10.2	13.8	16.7	19.2	24.0
7.5 mm Diameter	10.4	15.3	19.0	24.8	31.7	38.0
7.0 mm Diameter	15.6	21.8	27.0	33.5	41.9	48.9
6.5 mm Diameter	22.1	27.8	35.6	42.0	49.8	55.6

6.0 mm Diameter	24.0	31.7	37.2	45.9	53.0	58.2
5.5 mm Diameter	30.2	37.0	43.8	52.1	59.4	66.8
5.0 mm Diameter	33.8	42.4	48.0	57.5	63.1	69.9
4.5 mm Diameter	39.8	47.4	53.2	65.7	74.3	82.2

3.2 Laminar Flow and Velocity Profile Outline

To differentiate between laminar and turbulent flows in blood vessels, a dimensionless quantity known as Reynold's number represented by Re is very important. It relates the density (1.04 g/cm^3 and 1.067 g/cm^3 respectively for the two BMF samples), mean velocity and viscosity (4.3 mPa.s and 4.5 mPa.s respectively) of the fluid (BMF samples) with the diameter of the vessels.This number was calculated using equation 1 to be from 88.8 – 91.1 for phantom diameters of 4.5 mm – 8.0 mm for BMF with glucose, and 50.0 – 96.3 for phantom diameters of 4.5 mm – 8.0 mm for BMF with cholesterol. A Reynold's number of less than 2300 defines laminar flow, while a number higher than 4000 is characterized by a turbulent flow (Maulik, 2005; Azhim, 2015; Philip *et al.,* 2016; Peter *et al.,* 2019). Therefore, with our Reynold's number values less than 2300, it is established that the flow through the phantoms is laminar not turbulent(Carol & Deborah , 2017; Sandra, 2018).

Another important consideration was the entrance lengths at which the flows became laminar. These lengths were calculated using the equation (Nichols *et al.,* 2011):

$$L = 0.04 \times D \times R_e \quad \ldots\ldots 2$$

Where L is the entrance length and D is the diameter of the vessel. The values of L ranged from 1.6 cm to 2.9 cm in the 4.5 mm to 8.0 mm diameters for the first BMF and 1.6 cm to 1.7 cm in the 4.5 mm to 8.0 mm diameters for the second BMF. On an average, laminar flows were established at entrance length of 3 cm across all the diameters for both BMF with flow rate of 1500 ml/min. The velocity profile obtained from a phantom with a vessel diameter of 8.0 mm for both BMF is seen in figure 2 and figure 3 respectively. Other velocity profiles for 7.5 mm to 4.5 mm for both BMF samples can be seen in Appendices A1 and A2.

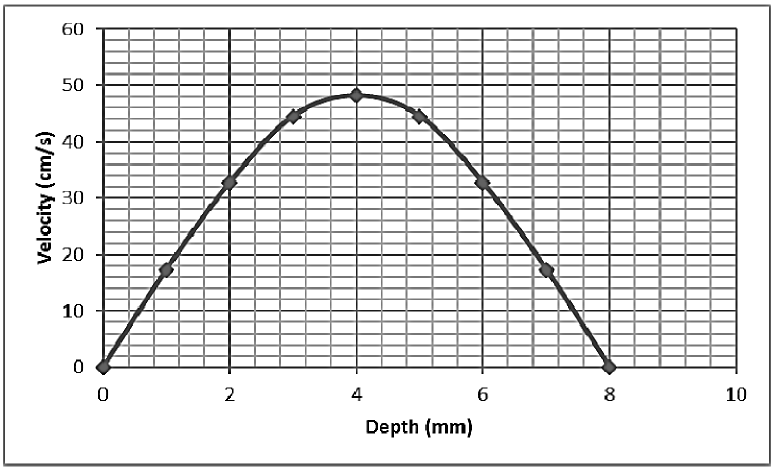

Figure 2: Velocity profile of BMF with glucose in the 8.0 mm wall-less phantom

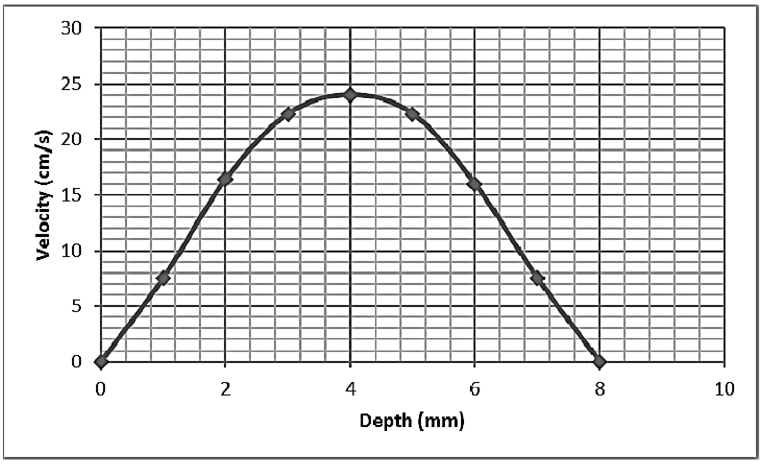

Figure 3: Velocity profile of BMF with cholesterol in the 8.0 mm wall-less phantom

The maximum velocities were located at the center of the vessel,decreasing to a minimum at the vessel walls. These velocity profiles fit the equation for parabola given in equation 3(Peter *et al.,* 2019)

$$y = aD^2 + bD + c \qquad \ldots\ldots\ldots\ldots 3$$

where y represents the mean velocity, D is the depth of measurement along the vessel's diameter, while a, b and c are constants. Therefore, we can say the flows are fully developed.

Conclusion

The research work was able to design, construct and characterized a multi-lumen diameter CCA wall-less phantom and BMF samples that mimics the real human vessels which were successfully used to study V_m in relation to flow rates, velocity profile and flow types. The velocity profiles and nature of flow found in this study are similar to those reported by in-vivo means. Since laminar flows and good velocity profiles were established across all lumens in the phantom in this research, we can conclude that studies on V_m, velocity patterns and flow types in the CCA can be studied using wall-less phantoms by Doppler ultrasound method.

Acknowledgment

We appreciate the support of all the authors providing technical support and editing of the manuscript. Dr. Pam S.D initiated the experiment and contributed in drafting of the manuscript. Dr. Dakok K.K, Dr. Sirisena and Mr. Nabasu Seth played vital roles in the manuscript drafting and also participated in prove reading the manuscript. All authors read and approved the final manuscript.

Financial support and sponsorship
Not applicable
Conflicts of interest
Not applicable

Reference

1. Ammar, A. O., Matjafri, M., Suardi, N., Oqlat, M. A., Oqlat, A. A., Abdelrahman, M. A., Farhat, O. F., Ahmad, M. S., Alkhateb, B. N., Gemanam, S. J., Shalbi, S. M., Abdalrheem, R., Shipli, M., Marashdeh, M. (2018). Characterization and Construction of a Robust and Elastic Wall-Less Flow Phantom for High Pressure Flow Rate Using Doppler Ultrasound Applications. *Natural and Engineering Sciences*, *3*(3), p.359–377.
2. Azhim, A. (2015). Exercise Improved Age-associated Changes in the Carotid Blood Velocity Exercise Improved Age-associated Changes in the Carotid Blood Velocity Waveforms. *Journal of Biomedical & Pharmaceutical Engineering*, 1(1), p.17–26.
3. Batten, J. R., & Nerem, R. M. (1982). Model study of flow in curved and planar arterial bifurcations. *Cardiovascular Research*, *16*(4), p.178–186.
4. Caro, C. G., Pedley, T. J., Schroter, R. C., Seed, W. A., & Parker, K. H. (2012). The Mechanics of the Circulation (2nd ed.), United Kingdom, Cambridge University Press.
5. Carol M. Rumack, D. L. (2017). Physics of Ultrasound. In *Diagnostic Ultrasound* (5th ed), Chicago, *E-book*. Elsevier Health Sciences, pp. 1–32.
6. Colquhoun, K., Alam, A., & Ã, D. W. (2005). Basic science : ultrasound. *Current Orthopaedics*, 19, p.27–33.
7. Correia, M., Provost, J., & Tanter, M. (2016). 4D ultrafast ultrasound flow imaging : in vivo quantification of arterial volumetric flow rate in a single heartbeat 4D ultrafast ultrasound flow imaging : in vivo quantification of arterial volumetric flow rate in a single heartbeat. *Physics in Medicine and Biology*, *61*, p.48–61.
8. Dakok K. K., Matjafri M. Z., Suardi N., Oglat A. A., Nabasu S. E. (2021). A blood-mimicking fluid with cholesterol as scatter particles for wall-less carotid artery phantom applications. J Ultrason; 21: e219–e224. doi: 10.15557/JoU.2021.0035
9. Hwang, J. Y. (2017). Doppler ultrasonography of the lower extremity arteries_ anatomy and scanning guidelines. *Ultrasonography*, *36*(2), p.111–119.
10. Kenwright, D. A., Laverick, N., Anderson, T., Moran, C. M., & Hoskins, P. R. (2015). Wall-less flow phantom for high-frequency ultrasound applications. In *Ultrasound in Medicine and Biology*, 41(3), pp.890–897.
11. Marrilee H., Judith H. (2020). Feline Diagnostic Imaging (1st Edition), USA, John Wiley & Sons, Inc.
12. Maulik, D. (2005). Doppler Ultrasound in Obstetrics and Gynecology (2nd ed.), New York, Springer Nature.
13. Nichols W. W., Michael F. O., Charalambos V., Arnold P. H. (2011). McDonald's Blood Flow in Arteries Theoretical, Experimental and Clinical Principles (6th ed.), USA, CRC Press.
14. Peter R. H., Kevin M., Abigail T. (2019). Diagnostic Ultrasound Physics and Equipment (3rd ed.), USA, CRC Press.
15. Philip M. Gerhart, Andrew L. Gerhart, J. I. H. (2016). Munson, Young and Okiishis Fundamentals of Fluid Mechanics (8th ed.). USA, Wiley.
16. Sandra L. H. (2018). Diagnostic Sonography (8th ed.). New York, Elsevier Mosby
17. Zhou, X., Kenwright, D. A., Wang, S., Hossack, J. A., & Hoskins, P. R. (2017). Fabrication of two flow phantoms for doppler ultrasound imaging. *IEEE Transactions on Ultrasonics, Ferroelectrics, and Frequency Control*, *64*(1), p.53–65.

List of Appendices

Appendix A1

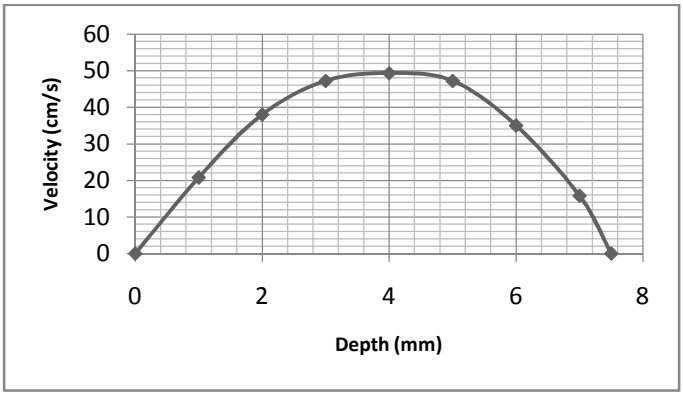

Figure A1(i): Velocity profile of BMF with glucose in the 7.5 mm wall-less phantom

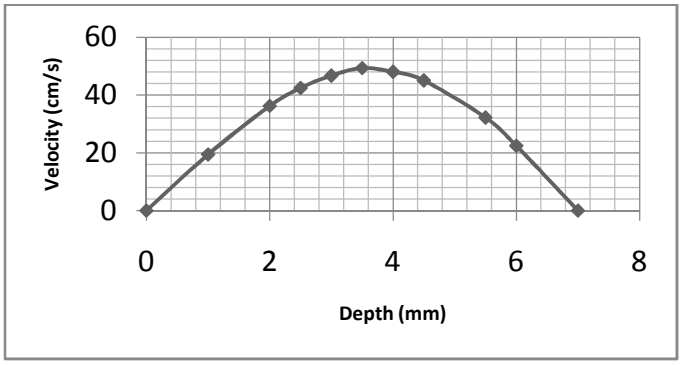

Figure A1(ii): Velocity profile of BMF with glucose in the 7.0 mm wall-less phantom

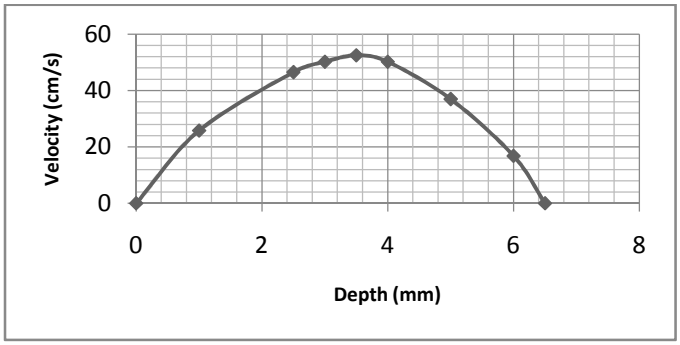

Figure A1(iii): Velocity profile of BMF with glucose in the 6.5 mm wall-less phantom

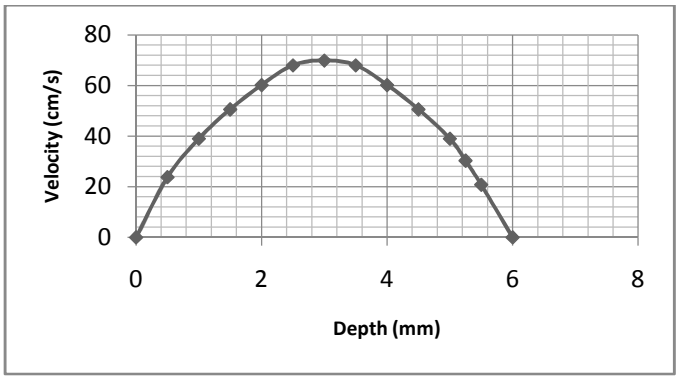

Figure A1(iv): Velocity profile of BMF with glucose in the 6.0 mm wall-less phantom

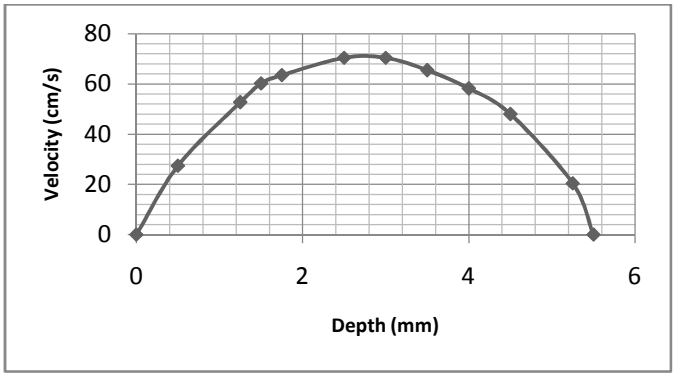

Figure A1(v): Velocity profile of BMF with glucose in the 5.5 mm wall-less phantom

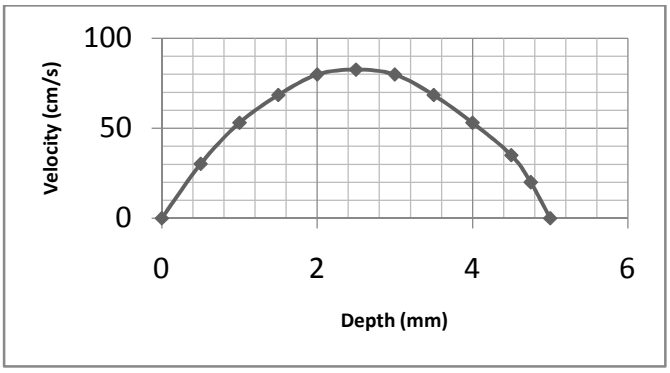

Figure A1 (vi): Velocity profile of BMF with glucose in the 5.0 mm wall-less phantom

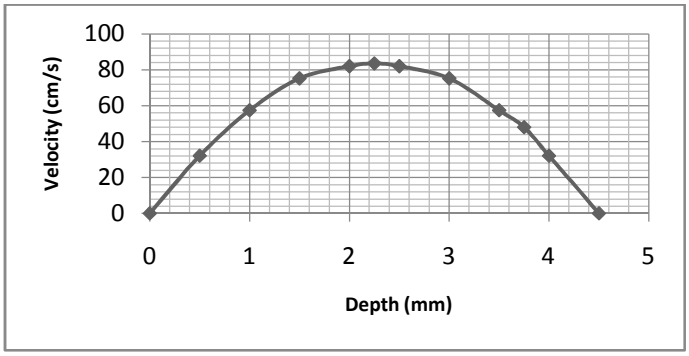

Figure A1 (vii): Velocity profile of BMF with glucose in the 4.5 mm wall-less phantoms

Appendix A2

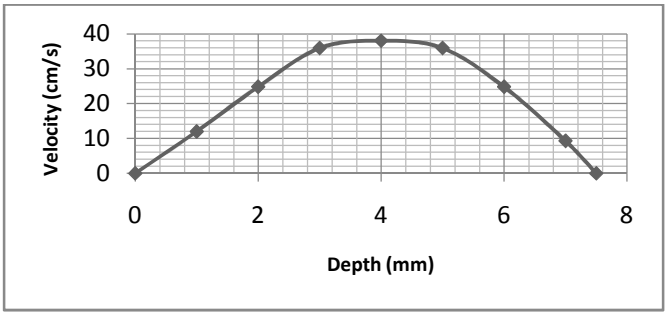

Figure A2(i): Velocity profile Of BMF with cholesterol In The 7.5 mm Wall-Less phantom

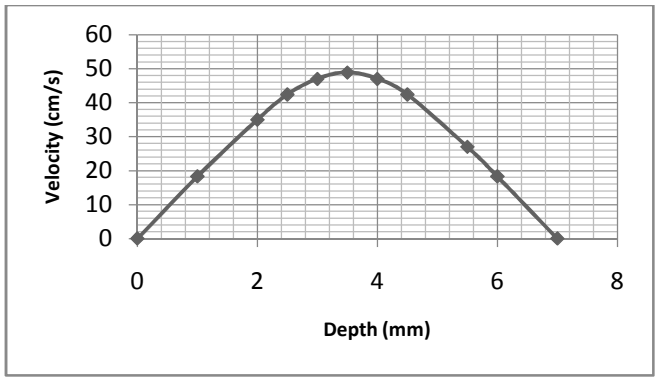

Figure A2 (ii): Velocity profile Of BMF with cholesterol In The 7.0 mm Wall-Less phantom

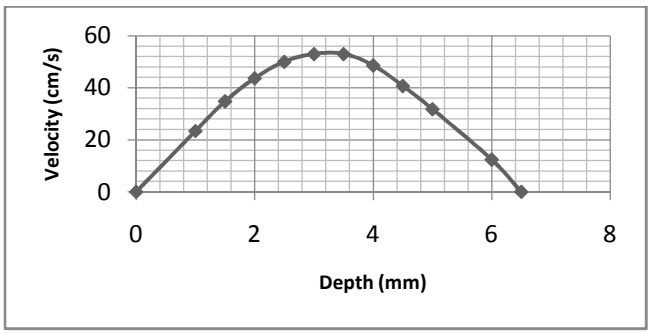

Figure A2 (iii): Velocity profile Of BMF with cholesterol In The 6.5 mm Wall-Less phantom

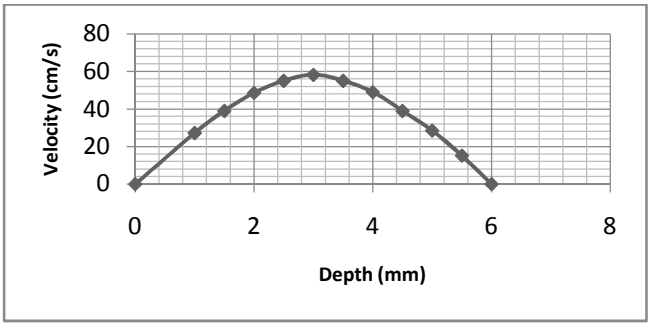

Figure A2(iv): Velocity profile Of BMF with cholesterol In The 6.0 mm Wall-Less phantom

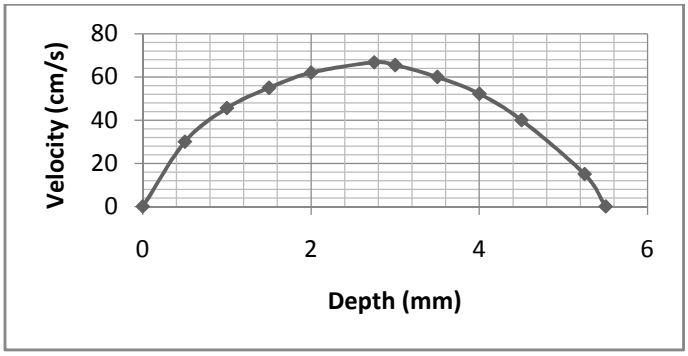

Figure A2 (v): Velocity profile Of BMF with cholesterol In The 5.5 mm Wall-Less phantom

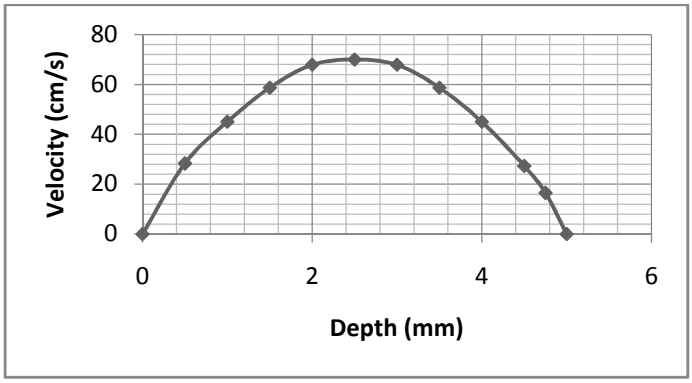

Figure A2 (vi): Velocity profile of BMF with cholesterol In The 5.0 mm Wall-Less phantom

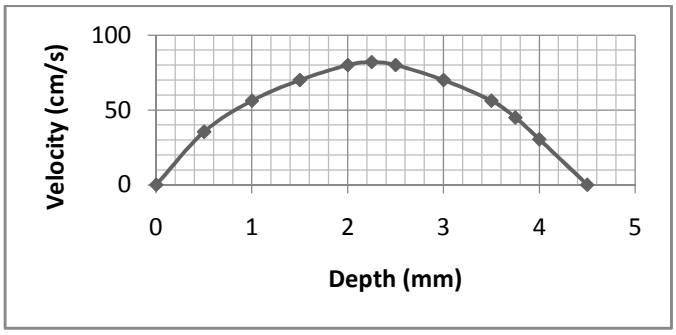

Figure A2(vii): Velocity profile of BMF with cholesterol In The 4.5 mm Wall-Less phantom